

# The Acoustical design of Mobile phones

**Yasuharu Onishi (1), Jun Kuroda (1), Yukio Murata (1), Motoyoshi Komoda (1),  
Kazuyuki Tsunoda (1), Yukio Yokoyama (2), Yasuhiro Oikawa (3),  
and Yoshio Yamasaki (3)**

(1) NEC CASIO Mobile Communications, Ltd., 1753 Shimonumabe, Nakahara-ku, Kawasaki-shi, Kanagawa 211-8666, Japan

(2) NEC Saitama Ltd., 300-18 Motohara, Kamikawa-cho, Kodama-gun, Saitama 367-0297, Japan

(3) Waseda University, 3-4-1 Okubo Shinjuku-ku, Tokyo 169-8555, Japan

**PACS: 43.38.FX (PIEZOELECTRIC AND FERROELECTRIC TRANSDUCERS) ,**

## ABSTRACT

In this paper, we describe the acoustic design used for mobile phones. Today's mobile phones provide a variety of audio capabilities, such as telephone communication, television, music, and movies. These capabilities are achieved by using acoustic devices such as receivers, speakers, and headphones. The most important of these devices are the speakers, which are used for almost all the audio functions of the mobile phone. However, today's mobile phones are much slimmer and more stylish than their predecessors, while maintaining a very high performance. The speakers used for these phones must be thin and small, but provide high-quality sound. Until now, the speakers used in mobile phones have had the problem of being too thick and difficult to mount. In this study, we analyzed the correlation between the acoustic structure of mobile phones and their acoustic properties and formulated design guidelines for achieving high-quality sound in slim mobile phones, which we also describe here.

## INTRODUCTION

Today's mobile phones provide a variety of audio capabilities, such as telephone communication, television, music, and movies. These capabilities are achieved by using acoustic devices such as receivers, speakers, and headphones. The most important of these devices are the speakers, which are used for almost all the audio functions of the mobile phone.

To achieve high-quality sound, mobile phone speakers must have a flat frequency response, adequate loudness, wide surround, and adequate directivity.

The design of the speakers must also suit today's more stylish mobile phones. Figure 2 shows the recent increase in demand for slim mobile phones. As can be seen in this figure, the thickness of mobile phones has been decreasing steadily over the past several years without affecting the performance.

These slim mobile phones require thin and small speakers that are easy to mount. To solve the problem of speaker thickness, we developed a 0.9-mm-thick piezoelectric speaker that consisted of a high-power bimorph transducer and an elastic support structure, and successfully used this ultrathin speaker in a slim mobile phone. However, the problem of mounting the speaker still remained. We therefore decided to establish a methodology for designing the speakers used in slim mobile phones.



**Figure 1 Acoustic devices used in mobile phones**

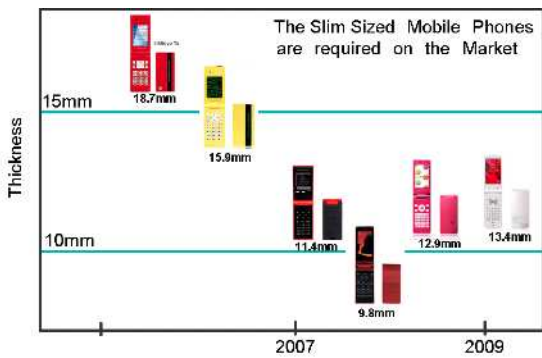


**Figure 2 Increase in demand for slim 3G mobile phones**

In this study, we analyzed the correlation between the acoustic structure of mobile phones and their acoustic properties in order to formulate design guidelines for achieving high-quality sound. For our experiment, we used mobile phones with 0.9-mm-thick piezoelectric speakers.

First, to clarify the route taken by the sound waves as they spread from the speaker to the LCD of the phone, we analyzed the directivity of the speaker. We were thereby able to formulate guidelines for designing the sound hole in the best position to maximize the sound pressure level at the LCD.

We then analyzed the effect of phone case vibration on the sound pressure level. By examining how phone case vibration caused the sound pressure level to decrease, we were able to formulate guidelines on damping phone case vibration.

Finally, we analyzed the correlation between the sound cavity (front cavity and back cavity) and the acoustic properties to understand how the acoustic structure of the phone affected its acoustic properties. We also optimized the method of calculating the sound characteristics by using equivalent circuit simulation to calculate the relationship between an estimated sound cavity and the acoustic properties in order to clarify our design guidelines.

## EXPERIMENT

### Speaker

We used the ultra-thin piezoelectric speaker shown in Figure 3 for this study. This ultra-thin piezoelectric speaker consisted of single-layer piezoceramics and shim materials and an elastic polymer and frame. Lead zirconate titanate (PZT) ceramics with a thickness of 40 μm were used as the piezoceramics. Both principal surfaces of the ceramics were covered by a silver electrode.

A phosphorate with a thickness of 0.5 μm was used as the shim material, and both principal surfaces of the phosphorate plate were covered by the piezoceramics. This was then used to construct a bimorph transducer.

An elastic polymer film was placed between the 0.9-mm-thick frame and shim, and the bimorph transducer was then attached to the frame. A 30-μm-thick polymer film was used as the elastic supporting material. All of the materials were connected by an adhesive and arranged in a concentric circle to create an ultra-thin speaker with a thickness of 0.9 mm.

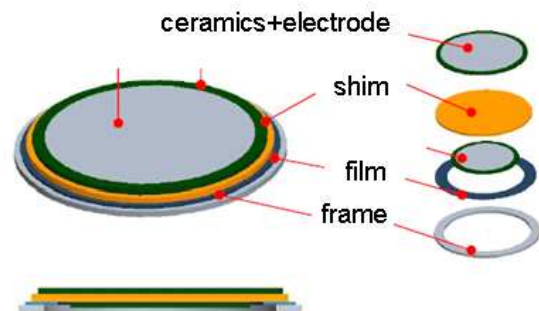


**Figure 3 Structure of ultra-thin speaker**

We made two kinds of speakers, one for a mobile phone with a front sound hole and one for a mobile phone with a side sound hole, and installed them in two mobile phones. The speakers are shown in Figure 4.

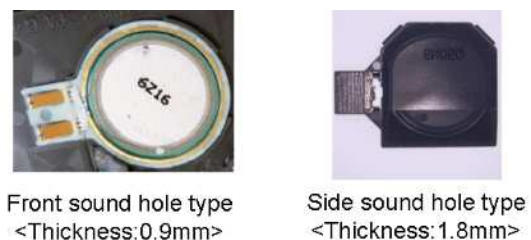


**Figure 4 Prototype speakers**

In the speaker for the mobile phone with a side sound hole, a cover was placed on the speaker vibration side. With this configuration, the sound reverberates off the cover and radiates out from the side of the speaker. The thickness of the speaker for the mobile with a front sound hole was 0.9 mm and the thickness of the speaker for the mobile phone with a side sound hole was 1.8 mm. Both of these speakers were thinner than an average electrodynamic speaker, which is about 3 mm thick.

## Mobile phone

The two kinds of mobile phones used—one with a front sound hole and one with a side sound hole—are shown in Figures 5 and 6. We used these mobile phones to evaluate the acoustic properties of the speakers.

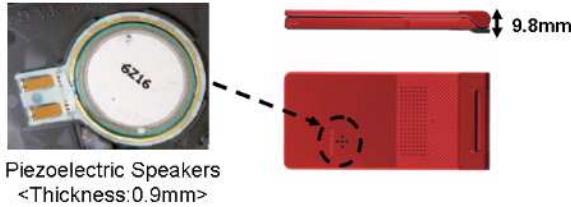


Figure 5 Mobile phone with front sound hole

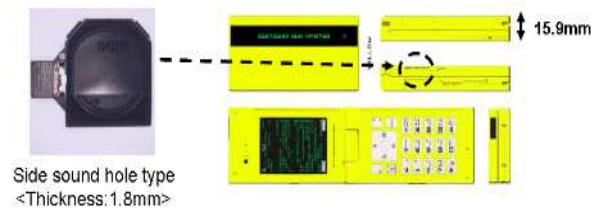


Figure 6 Mobile phone with side sound hole

## Measurements

### • Electrical properties

The electric properties of the speakers, such as the resonant frequency and electrostatic capacity ( $C_p$ ), were measured by using a Hewlett-Packard impedance analyzer (4194A).

The values of  $Q_m$  and the equivalent circuit constants for the transducers were measured at a low vibration level by measuring the impedance-frequency responses by using a Hewlett-Packard impedance analyzer (4194A). The  $Q_m$  of the transducers was defined by equation (1) below [15].

$$Q_m = \frac{F_s}{f_2 - f_1} \quad (1)$$

Where  $f_s$  represents the resonant frequency and  $f_1$  and  $f_2$  represent the quadrantal frequencies.

### • Acoustic properties

The acoustic properties of the speakers were measured by using an audio analyzer. The distance between the centre of the sound hole in the mobile

phone and the microphone of the audio analyzer was 10 cm. A driving voltage of 5 V<sub>rms</sub> was input to the speakers. The frequency bandwidth was 100 Hz to 20 kHz. The acoustic properties were measured in an anechoic room.

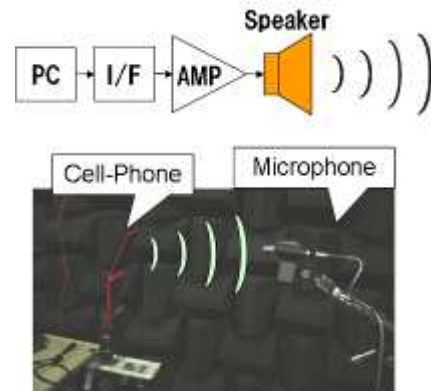


Figure 7 Method used to measure the acoustic properties of the speakers

The directivity characteristics were measured by using a rotating table in an anechoic room. We centered the mobile phone on the table and rotated the table 360 degrees, measuring the acoustic properties at ten-degree intervals (36 measurements).

### • Vibration properties

We measured the vibration of the mobile phone by using a vibrometer. The distance between the mobile phone and the scan-head was 30 cm. A driving voltage of 5 V<sub>rms</sub> was input to the speakers and the frequency bandwidth was 100 Hz to 20 kHz.

## RESULTS AND DISCUSSION

### Location of sound hole

We examined the effect of the mobile phone's sound hole position on the acoustic properties by using the two kinds of mobile phones—one with a front sound hole and one with a side sound hole—shown in Figures 5 and 6.

To eliminate the effect of phone case vibration, we placed damping materials on the surface of the phone cases of the mobile phones. We then evaluated the directivity of the sound in the mobile phones.

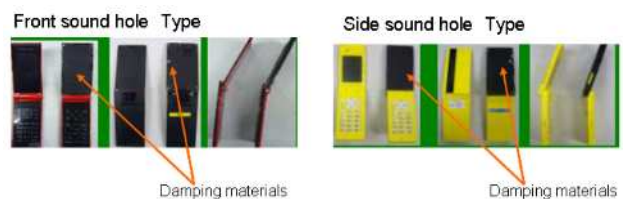
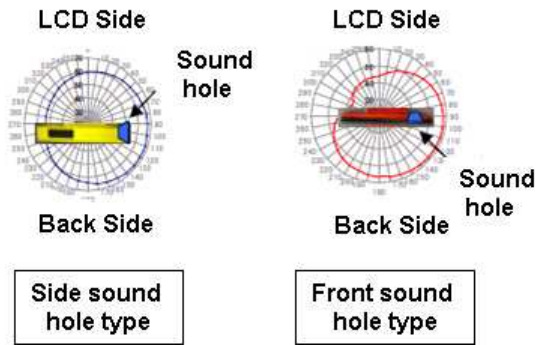


Figure 8 Mobile phones with damping materials

We analyzed the direction in which the sound waves from the speakers in the two kinds of mobile phones dispersed. The distance between the center of the phone case and the microphone was 10 cm. We rotated the phone case 360 degrees, measuring the directivity characteristics from the center of the phone every ten degrees. Figure 9 shows the position of the mobile phones in the directivity analysis.



**Figure 9** Position of mobile phones in directivity analysis

Figure 10 shows the directivity characteristics at each frequency. We set up the mobile phones to play back a movie and evaluated the difference in the sound pressure level between the speaker location and the LCD of the phone. Specifically, we analyzed the attenuation of the sound pressure level when the sound wave moved from the sound hole to the LCD.

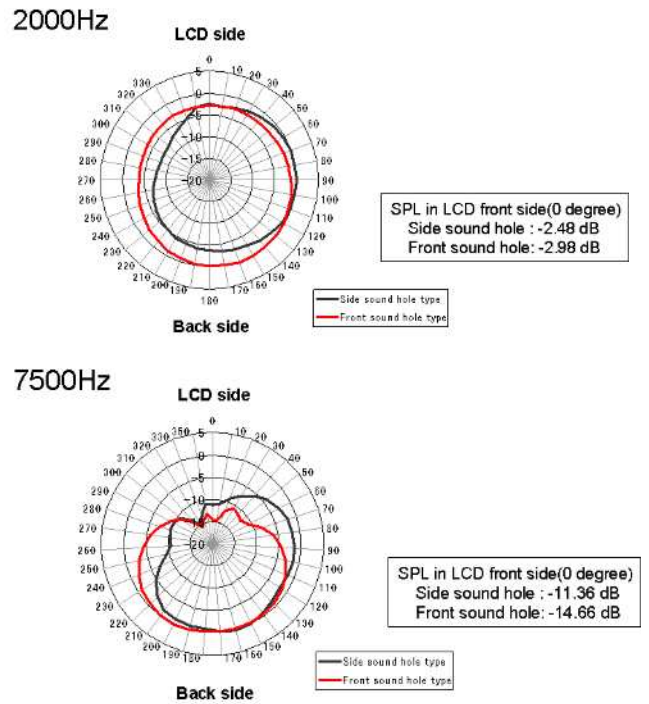


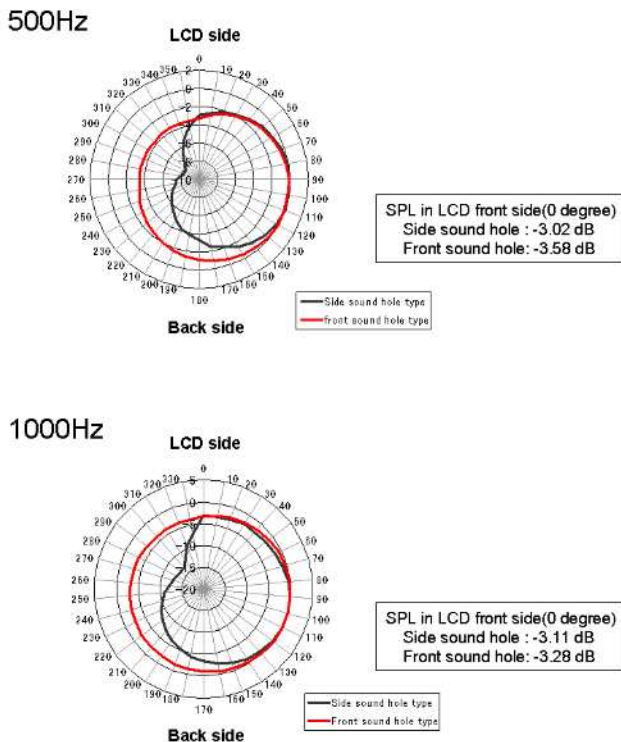
**Figure 10** Directivity analysis of mobile phones

In a low-frequency bandwidth of 2000 Hz or less, the attenuation of the sound pressure level at the LCD was 5 dB or less in both mobile phones. On the other hand, the attenuation of the sound pressure level at the LCD was 10 dB or more at 7500 Hz. We assumed that this was because the sound waves were muffled by the phone case. We therefore proposed moving the sound hole closer to the LCD to enable support for applications in the high-frequency band with strong directivity.

Next, we compared the directivity characteristics of the two mobile phones. In a low-frequency bandwidth of 2000 Hz or less, the attenuation of sound pressure level in the mobile phone with the front sound hole was similar to that in the phone with a side sound hole (3 dB or more).

However, the directivity characteristics of the phone with a side sound hole had a slightly distorted shape compared with those of the phone with a front sound hole. In the phone with a side sound hole in particular, the attenuation of the sound pressure level in the area opposite to the sound hole was larger, due, we assumed, to the muffling of the sound waves by the phone case.

Next, we examined the acoustic properties of the phone with a front sound hole in detail by using a sound simulator. The effect of the sound hole position was analyzed by using the analytical model shown in Figure 11.



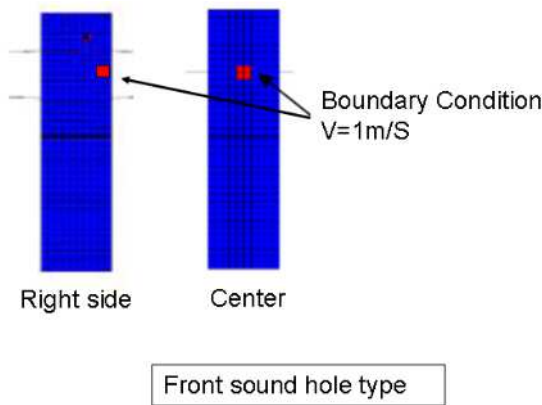


**Figure 11 Simulation model used in directivity analysis**

We moved the sound hole position in the mobile phone with a front sound hole right and left and compared the attenuation of the sound pressure level at the LCD. Figure 12 shows the results. The sound hole that was closest to the LCD had the least sound pressure level attenuation. Moreover, the sound pressure level in decibels attenuated significantly at 7500 Hz, which corresponds to the results of the experiment above.

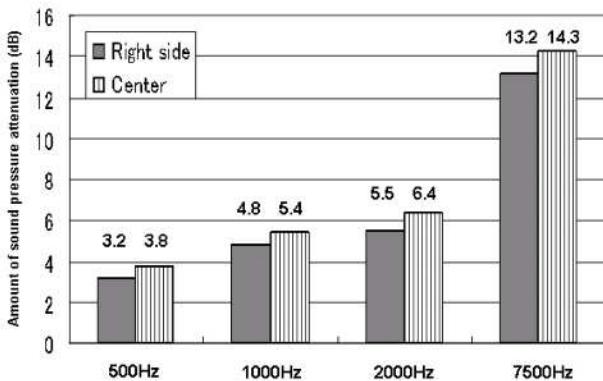


**Figure 12 Sound pressure level (SPL) attenuation**

We then analyzed the route taken by the sound waves as they spread from the speaker to the LCD. In the low-frequency bandwidth, the pressure of the sound from the speaker attenuated by about 3 to 5 dB. However in the high-frequency bandwidth with high directivity, the attenuation was 10 dB or more. We assume that this was because the sound waves were muffled by the phone case. Through this analysis, we could see that the dispersion of the sound waves changes considerably depending on where the sound hole is located. We were therefore able to clarify that the muffling of the sound waves by the phone case meant that it was important to consider the position of the sound hole when designing the mobile phone.

## Effect of phone case vibration

We analyzed the effect of phone case vibration on the sound pressure level by measuring the acoustic properties of the two kinds of mobile phones with and without damping materials. The damping materials were placed on the surface of the phone case in both phones. Tables 1 and 2 show the results of measuring the sound pressure level (SPL) at the sound hole and at the LCD.

**Table 1 SPL change at sound hole**

	Side sound hole type			Front sound hole type		
	None	Damping material	Amount of attenuation	None	Damping material	Amount of attenuation
500Hz	64.9 dB	68.8 dB	-3.5 dB	60.4 dB	68.1 dB	-7.7 dB
1000Hz	81.6 dB	85.6 dB	-3.7 dB	87.0 dB	76.7 dB	-9.5 dB
2000Hz	80.0 dB	79.8 dB	-0.4 dB	85.3 dB	82.5 dB	+2.2 dB
7500Hz	85.6 dB	84.4 dB	-1.2 dB	97.7 dB	102.6 dB	+4.9 dB

Amount of attenuation = SPL (Damping material) - SPL (none)

**Table 2 SPL change at LCD**

	Side sound hole type			Front sound hole type		
	None	Damping material	Amount of attenuation	None	Damping material	Amount of attenuation
500Hz	69.9 dB	64.9 dB	-6.0 dB	52.6 dB	63.2 dB	-10.6 dB
1000Hz	80.7 dB	78.6 dB	-2.1 dB	69.8 dB	79.6 dB	-9.8 dB
2000Hz	79.8 dB	76.9 dB	+3.0 dB	74.8 dB	77.0 dB	-2.2 dB
7500Hz	80.7 dB	81.5 dB	+0.8 dB	81.2 dB	81.2 dB	-0.2 dB

Amount of attenuation = SPL (Damping material) - SPL (none)

In both the mobile phones, phone case vibration caused the sound pressure level to attenuate significantly at  $F_0$  or less. The resonant frequency is about 500 to 1000 Hz because a material that includes resin is used for the phone case.

We decided that it was possible that a sound wave generated by phone case vibration caused by driving the speaker was interfering with the sound wave from the speaker. Because the phone case vibrates considerably at the resonant frequency of the case, the generated sound wave is large. We assumed that the sound wave from the phone case and the sound wave from the speaker interfered at opposite phases, canceling each other out and causing the sound pressure level to attenuate.

At 2000 Hz or more, the sound pressure level increased and decreased according to the sound hole position and the direction of measurement. The phone case generated a distributed vibration mode in a high-frequency bandwidth. We assumed that the sound waves repeatedly interfered and canceled each other out due to phase changes in a limited part of the phone case.

Next, we analyzed the effect of phone case vibration on sound pressure level attenuation in detail. Figure 13 shows these results.

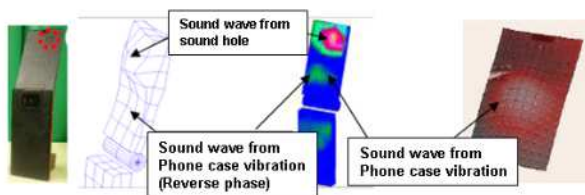


**Figure 13** Analysis of sound pressure distribution and vibration mode

Here, we analyzed the sound pressure distribution and vibration mode of the phone case. We could thereby clarify the generation of the sound wave caused by phone case vibration. We could also clarify that the phase of the sound wave from the speaker and the phase of the sound wave from the phone case were reversed, and that these sound waves canceled each other out.

Using this analysis, we could show that phone case vibration had a large effect on sound pressure level attenuation. The attenuation of the sound pressure level was particularly large in the low-frequency bandwidth near the resonant frequency of the phone case. The sound wave from the speaker was canceled out by the sound wave from the phone case. It is therefore clear that measures to reduce the vibration of the phone case are necessary to achieve high-quality sound.

**Effect of acoustic cavity**

We analyzed how different speaker installations affected the acoustic properties of the mobile phone by evaluating the correlation between the acoustic properties, the sound hole location, and the acoustic cavity (front cavity and back cavity). We analyzed the conductance frequency response by using the mobile phone with a front sound hole. We measured the change in the fundamental resonant frequency and the change in the sound pressure level. The analyzed samples are shown in Figure 14.

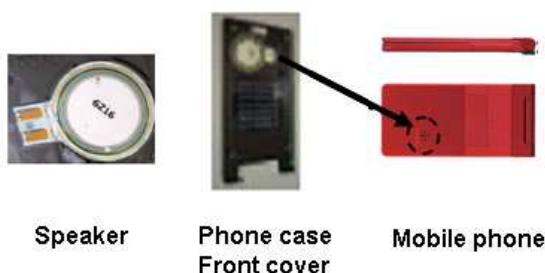


**Figure 14** Analyzed samples

We measured the speaker unit and the front cover in which the speaker was installed. The size of the front cavity was 0.5 cc and the size of the back cavity was 0.1 cc. We measured the speaker unit by itself, the speaker unit installed in the front cover with a sound hole and a back cavity, and the speaker unit installed in a mobile phone with a sound hole and a front and back cavity. We estimated the proportion of the current value and the sound particle velocity, and roughly estimated the attenuation of the sound pressure level caused by the change in conductance. Tables 3 and 4 show the results of this analysis.

**Table 3** Effect of acoustic cavity in mobile phone with side sound hole

	500Hz	F0		2000Hz	7500Hz
Speaker	—	946Hz	—		
Front cover	-2.9dB	916Hz	-3.4dB	+0.1dB	-0.2dB
Mobile phone	-6.8dB	896Hz	-7.3dB	+0.2dB	+0.3dB

Amount of attenuation = SPL - SPL (speaker)  
 F0: Fundamental resonant frequency

**Table 4** Effect of acoustic cavity in mobile phone with front sound hole

	500Hz	F0		2000Hz	7500Hz
Speaker	—	996Hz	—		
Front cover	-2.7dB	945Hz	-2.5dB	-2.8dB	-0.9dB
Mobile phone	-8.4dB	896Hz	-11.2dB	-7.5dB	-1.9dB

Amount of attenuation = SPL - SPL (speaker)  
 F0: Fundamental resonant frequency

The fundamental resonant frequency of the speaker unit decreased due to the sound hole, the front cavity, and the back cavity. The mechanical quality factor ( $Q_m$ ) also tended to decrease. When there was a back cavity, the mechanical quality factor ( $Q_m$ ) decreased remarkably. The sound pressure level also tended to decrease as the fundamental resonant frequency and quality factor ( $Q_m$ ) decreased.

We assumed that this was due to an increase in acoustic inertia and the effect of pressure loss. We also assumed that the effect of the back cavity was large because the volume of air was particularly small.

On the other hand, it seems that the change in the sound pressure level is smaller, and the effect of acoustic inertia and pressure loss is less in a high-frequency bandwidth.

Next, we developed a method to optimize the sound characteristics by using equivalent circuit simulation to examine the correlation between design factors and acoustic properties so that we could formulate guidelines for designing the

acoustic cavity (front cavity and back cavity). Figure 15 shows the equivalent circuit model that we used.

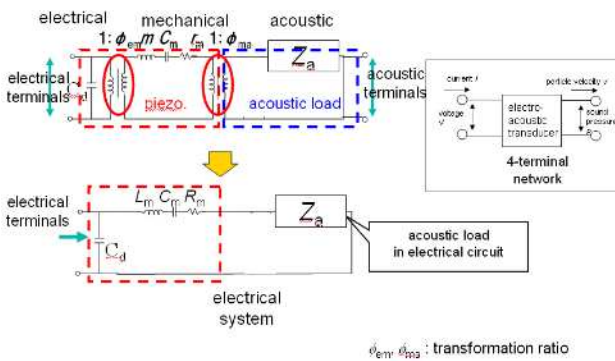


**Figure 15** Equivalent circuit simulation model

**Table 5** Calculation of acoustic properties by changing size of back cavity

Back cavity (CC)	F <sub>0</sub> (Hz)	SPL (500Hz) dB	SPL (F <sub>0</sub> ) dB	SPL (2kHz) dB
0.10	3150	55.6	111.3	84.3
0.25	2470	59.5	107.4	92.5
0.50	2020	63.1	102.8	102.7
0.75	1670	64.7	99.7	99.6
1.00	1420	66.7	97.5	95.5
2.00	1320	69.8	96.7	92.1
3.00	1270	71.2	96.5	91.1
4.00	1260	72	96.4	90.5
5.00	1240	72.6	96.2	90.3
7.50	1210	73.2	95.5	90.0
10.00	1180	73.9	95.2	89.7

**F<sub>0</sub>: Fundamental resonant frequency**

As the size of the back cavity decreases, the fundamental resonant frequency increases, and the sound pressure level decreases. In the low-frequency bandwidth in particular, the attenuation of the sound pressure level is large. For example, when the size of the cavity is reduced to 0.5cc or less, the sound pressure level is about 10 dB lower than the level when the cavity is 10 cc at 500 Hz. It is therefore likely that the sound pressure level will decrease considerably in a thin mobile phone with small back cavity. The acoustic cavity is therefore an important design factor in achieving high-quality sound in the slim mobile phones to be developed from now.

**SUMMARY**

As mobile phones become thinner, greater restrictions are placed on how the speakers are mounted. It is also necessary to improve the phone's acoustic capabilities to achieve the high sound quality required by today's mobile phones.

The aim of this study was to formulate design guidelines to help achieve high sound quality in slim mobile phones.

To achieve this, we studied the route the sound waves took as they dispersed from the speaker and the effect of phone case vibration on sound pressure level attenuation. We also looked at the correlation between the sound cavity and the acoustic properties.

**CONCLUSION**

- In terms of the sound wave dispersion route, the sound pressure level attenuation at the LCD in the front was larger in the high-frequency bandwidth. Moreover, the directivity properties changed according to the sound position. We determined that this was due to the muffling of the sound waves by the phone case. It is therefore necessary to design the sound hole position taking the phone case structure into account.
- Phone case vibration had a large effect on sound pressure level attenuation. Attenuation was especially large in the low-frequency bandwidth. We determined that the sound waves from the phone case canceled out the sound waves from the speaker. It is therefore important to take steps to control phone case vibration in a slim mobile phone.
- Concerning the correlation between the acoustic cavity and the acoustic properties, we found that the sound pressure level attenuated as the acoustic cavity became smaller. This was especially true in mobile phones with a small cavity. In a slim mobile phone, therefore, it is important to design the sound cavity carefully.

Using these results, we were able to understand the correlation between the design factors and the acoustical properties in slim mobile phones and formulate appropriate acoustic design guidelines.

## REFERENCES

- [1] S. Takahashi and S. Hirose, "Vibration-level characteristics of lead zirconate titanate ceramics," *Jpn. J. Appl. Phys.*, vol. 31, pp. 3055-3057, Sept. 1992.
- [2] S. Takahashi and S. Hirose, "Vibration-level characteristics for iron-doped lead zirconate titanate ceramic," *Jpn. J. Appl. Phys.*, vol. 32, pp. 2422-2425, May 1993.
- [3] S. Takahashi, S. Hirose, and K. Uchino, "Stability of PZT piezoelectric ceramics under vibration level change," *J. Am. Ceram. Soc.*, vol. 77, pp. 2429-2432, Sept. 1993.
- [4] S. Takahashi, S. Hirose, K. Uchino, and K. Y. Oh, "Electro-mechanical characteristics of lead zirconate titanate ceramics under vibration-level change," *Proceeding of the 9th IEEE Int'l Symp. Appl. Ferroelectrics*, 1994, pp. 377- 382.
- [5] S. Takahashi, Y. Sasaki, S. Hirose, and K. Uchino, "Stability of  $\text{PbZrO}_3\text{-PbTiO}_3\text{-Pb}(\text{Mn}_{1/3}\text{Sb}_{2/3})\text{O}_3$  piezoelectric ceramics under vibration-level change," *Jpn. J. Appl. Phys.*, vol. 34, pp. 5328-5331, Sept. 1995.
- [6] S. Takahashi, M. Yamamoto, and Y. Sasaki, "Nonlinear piezoelectric effect in ferroelectric ceramics," *Jpn. J. Appl. Phys.*, vol. 37, pp. 5292-5296, Sept. 1998.
- [7] M. Umeda, K. Nakamura, and S. Ueha, "The measurement of high-power characteristics for a piezoelectric transducer based on the electrical transient response," *Jpn. J. Appl. Phys.*, vol. 37, pp. 5322-5325, Sept. 1998.
- [8] M. Umeda, K. Nakamura, and S. Ueha, "Effects of vibration stress and temperature on the characteristics of piezoelectric ceramics under high vibration amplitude levels measured by electrical transient responses," *Jpn. J. Appl. Phys.*, vol. 38, pp. 5581-5585, Sept. 1999.
- [9] S. Takahashi, Y. Sasaki, M. Umeda, K. Nakamura, and S. Ueha, "Nonlinear effect of piezoelectric resonators," *Tech. Rep. Institute of Electrical Engineers in Japan*, MM-00-10, pp. 7-12, March 2000. [in Japanese]
- [10] M. Umeda, S. Takahashi, Y. Sasaki, K. Nakamura, and S. Ueha, "Vibration stress and temperature dependence of piezoelectric resonators with lead-zirconate-titanate ceramics," *Trans. Institute of Electronics, Information and Communication Engineers C-I*, vol. J82-C-I, pp. 762-768, Dec. 1999. [in Japanese]
- [11] S. Takahashi, Y. Sasaki, M. Umeda, K. Nakamura, and S. Ueha, "Characteristics of piezoelectric ceramics at high vibration level," in *Proceeding of the Mater. Res. Soc. Symp.*, 1999. (in press)
- [12] S. Takahashi, Y. Sasaki, M. Umeda, K. Nakamura, and S. Ueha, "Measurement of piezoelectric properties using composite-bar method," *Tech. Rep. Institute of Electrical Engineers in Japan*, MM-00-11, pp. 13-18, March 2000. [in Japanese]
- [13] H. Kawai, Y. Sasaki, T. Inoue, T. Inoi, and S. Takahashi, "High-power transformer employing piezoelectric ceramics," *Jpn. J. Appl. Phys.*, vol. 35, pp. 5015-5017, Sept. 1996.
- [14] S. Takahashi, Y. Sasaki, S. Hirose, and K. Uchino, "Electro-mechanical properties of  $\text{PbZrO}_3\text{-PbTiO}_3\text{-Pb}(\text{Mn}_{1/3}\text{Sb}_{2/3})\text{O}_3$  ceramics under vibration-level change," in *Proceeding of the Mater. Res. Soc. Symp.*, vol. 360, pp. 305- 310, 1995.
- [15] T. Ikeda: *Fundamentals of Piezoelectricity* (Oxford Science Publications, Oxford, New York, Tokyo, 1996).